

Fractal Growth of Two-Dimensional Islands: Au on Ru(0001)

R. Q. Hwang, J. Schröder, C. Günther, and R. J. Behm

*Institut für Kristallographie und Mineralogie, Universität München,
Theresienstrasse 41, W-8000 München 2, Federal Republic of Germany*
(Received 19 March 1991)

The two-dimensional growth of Au on Ru(0001) in the submonolayer range has been investigated with scanning tunneling microscopy. Upon deposition at room temperature, highly dendritic islands of one layer thickness grow on large Ru terraces. These irregular island shapes are removed upon annealing to 650 K. The dendritic islands exhibit a fractal character, and a dimensional analysis yields a fractal dimension of 1.72 ± 0.07 . The results are in quantitative agreement with a two-dimensional diffusion-limited-aggregation growth mechanism.

PACS numbers: 68.55.Gi, 61.16.Di, 68.70.+w

The physics of thin-film growth is a topic of much current interest. With improvements in the spatial resolution of surface science techniques, such as electron microscopy methods and scanning tunneling microscopy (STM), details of the film growth and morphology can be studied. Recent investigations have uncovered novel and intriguing phenomena, pointing to the importance of kinetics in film growth [1-4]. We report on first results of an extensive STM investigation on the growth of Au films on Ru(0001) in which the film morphology has been systematically studied under various growth conditions. In the submonolayer range, only monolayer clusters form. The effects of kinetics and defects on the nucleation behavior can be clearly seen [5], which will be discussed in detail in a forthcoming paper. In this Letter we concentrate on the mechanism of 2D growth in the submonolayer range, where monolayer islands are formed over a wide coverage range. Upon deposition at room temperature, the islands exhibit highly dendritic shapes. We believe their formation is a striking example of a two-dimensional diffusion-limited-aggregation process [6,7]. To verify this, we have studied the effects of annealing on these films as well as confirmed the expected fractal nature of the island shapes.

The measurements were made in a UHV chamber equipped with facilities for standard surface analysis techniques, such as Auger spectroscopy (AES), low-energy electron diffraction (LEED), thermal desorption spectroscopy (TDS), in addition to a "louse"-type STM [8]. Details of the sample preparation are given elsewhere [5]. Au was evaporated from a resistively heated tungsten filament positioned 11 cm from the sample, thus providing uniform deposition across the 6-mm Ru(0001) sample. Incident Au flux rates ranging from 0.2 to 2 ML/min (ML denotes monolayer) were used. All depositions were performed at room temperature. Au coverages were determined by a combination of AES, TDS, and STM. STM images recorded in the constant-current mode at typically 100- to 500-mV tunnel voltage and 0.25- to 2-nA tunnel current are displayed in a top-view representation with dark regions corresponding to lower levels.

Examples of the island growth at room temperature as a function of coverage are shown in the series of images in Figs. 1(a)-1(d). The incident flux was identically 1.8 ML/min for all four films. Already at the lowest coverage of 0.03 ML, 2D Au islands are seen to nucleate [Fig. 1(a)]. The smaller islands have quite compact shapes with diameters of 100 to 200 Å. The larger islands in this image show beginnings of armlike growth extending from a core of similar size. These arms also exhibit a characteristic width of approximately 100 Å. A higher-coverage film of 0.15 ML is imaged in Fig. 1(b). Many islands are visible on several Ru terraces. The growth is seen to continue in a dendritic or irregular pattern while maintaining an arm width of about 100 Å. At a still higher coverage of 0.37 ML, the dendritic shapes are even more pronounced [Fig. 1(c)]. At this coverage, a noticeable amount of thickening has occurred in the island arms. This can be explained by two effects. First, at higher coverages, a larger fraction of the deposited Au impinge onto existing islands. These adatoms can diffuse off of the first layer islands and condense at the step edge, thereby thickening the structure. In addition, as the linear sizes of the islands become larger, a higher percentage of the bare Ru makes up the "fjord" areas between the arms. Au atoms in these regions tend to fill in these fjords and do not contribute to further radial growth. These effects are even more obvious at higher coverages [Fig. 1(d)]. At 0.69 ML, most of the ramified structure observed at lower coverages has now been lost. The radial growth, on the other hand, was slowed to the extent that the islands have not coalesced and can still be identified as individual entities.

The dendritic shapes are due to kinetic limitations existing at room temperature which can be concluded from their thermal instability. Figure 2(a) shows an image of the film of Fig. 1(c) after annealing briefly to 650 K. The distribution and populations of the islands remain unaffected by the heating, but clear changes in their morphology are apparent. The islands have collapsed into much more compact forms. Heating to 1100 K leads to even more drastic changes, as shown in Fig. 2(b). The islands have now coalesced into large connected structures

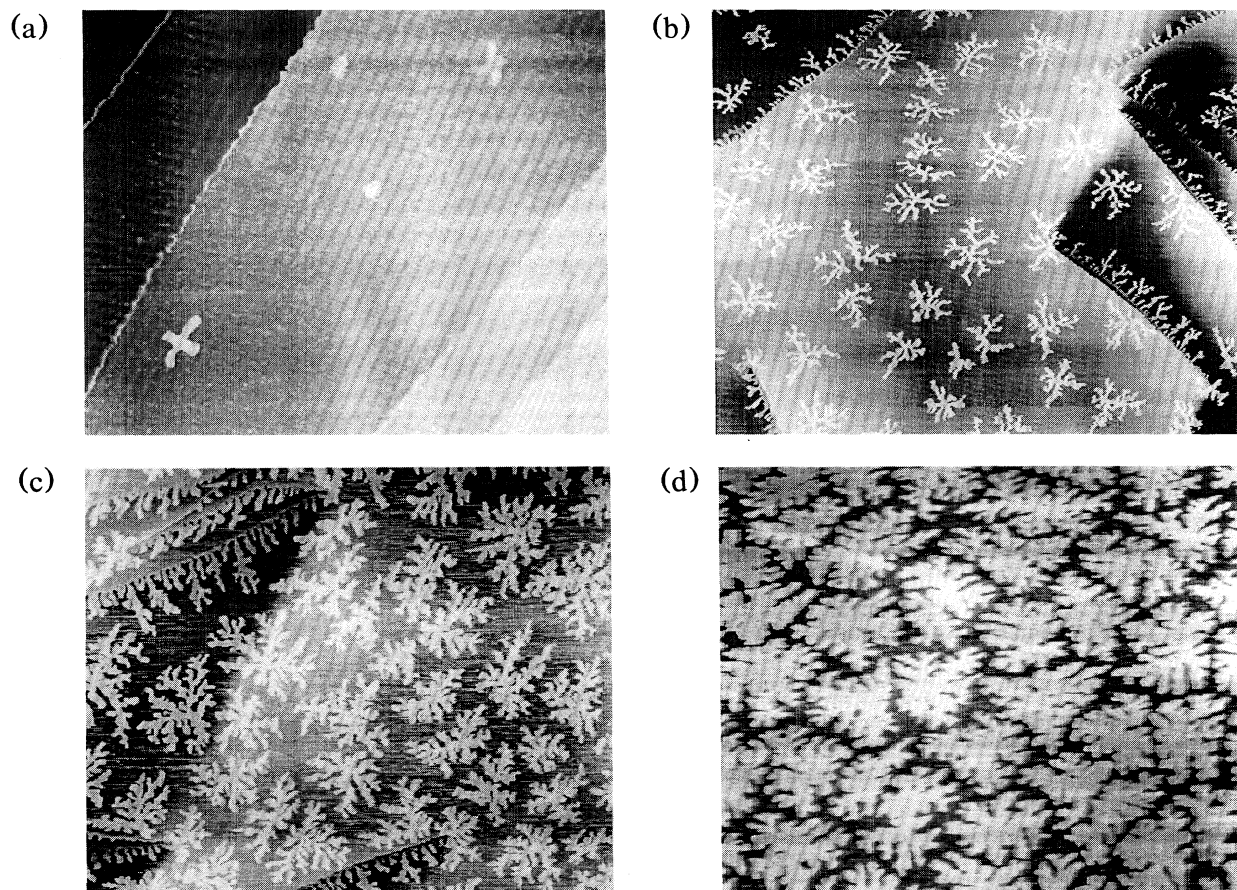


FIG. 1. Images of four films of varying coverages deposited at room temperature with a flux of 1.8 ML/min. (a) $\Theta=0.03$ ML ($0.70 \mu\text{m} \times 0.60 \mu\text{m}$), (b) $\Theta=0.15$ ML ($1.31 \mu\text{m} \times 1.20 \mu\text{m}$), (c) $\Theta=0.37$ ML ($1.13 \mu\text{m} \times 0.96 \mu\text{m}$), (d) $\Theta=0.69$ ML ($1.32 \mu\text{m} \times 1.13 \mu\text{m}$).

many thousands of angstroms in size. From these data we conclude that upon annealing to 650 K, Au atoms can migrate along island edges leading to smoother structures. They cannot, however, dissolve from the cluster; hence there is little mass transfer between Au islands. In contrast, heating to 1100 K evaporates the Au islands into a 2D lattice gas followed by recondensation during cooling, forming extended connected structures.

This suggests that the dendritic forms grown at room temperature are intimately related to the restricted diffusion of Au atoms once they are condensed at the edge of an island. The large distance between nuclei, on the other hand, implies that individual Au atoms are highly mobile under these conditions. Models of crystal growth considering these effects have been extensively studied within diffusion-limited-aggregation (DLA) [6,7] and associated models [9–12]. These models have attracted much recent theoretical attention due to their relationship to fractal growth and critical phenomena. In their original DLA model, Witten and Sander [7,8] simu-

lated two-dimensional growth by injecting atoms onto a lattice very far from a seed cluster at its center. The atoms then performed random walks until they encountered the cluster or traveled off the lattice field. Once attached to the cluster, however, the atoms were trapped, with no further diffusion. Clusters formed in this way were highly dendritic. They were also shown to possess the property of self-similarity with a Hausdorff or fractal dimension $D=1.70 \pm 0.02$. Relaxing the assumptions of this model in various ways, e.g., by allowing nonunity sticking coefficient to the cluster or by considering other lattice symmetries, had no effect on the resulting fractal dimension; i.e., D appeared to be universal [7,12]. Variations on this model have also been studied. Meakin [11] modified the model by allowing clusters to also diffuse. Structures formed in this way also exhibited fractal behavior but with a fractal dimension between 1.45 and 1.5. Others have considered the case in which the diffusing particles traveled in straight trajectories instead of performing random walks and go under the names “ballistic

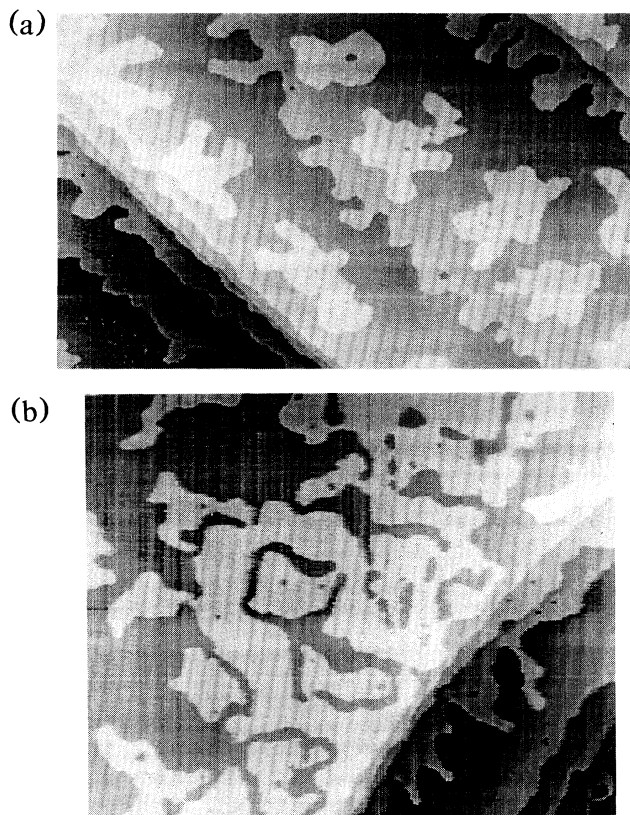


FIG. 2. Images of the identical film shown in Fig. 1(c) after annealing to (a) 650 K ($0.83 \mu\text{m} \times 0.54 \mu\text{m}$) and (b) 1100 K ($0.76 \mu\text{m} \times 0.66 \mu\text{m}$).

aggregation" and "random rain." Though this type of growth produced open structures, they were found to be nonfractal with the trivial dimension $D=2$ [9,10].

To check the applicability of these models to the growth of 2D Au clusters, we have performed a dimensional analysis following Ref. [12]. Fractal behavior would imply a power-law dependence of the cluster size N with its radius of gyration R_g of the form

$$N \sim R_g^D.$$

To analyze our experimentally grown clusters, subsets of the clusters were defined by concentric circles about the island center. N and R_g were then computed for each subset.

In applying such an analysis, power-law behavior can only be expected in a limited range of R_g . To smaller lengths, the fitting range is limited by the arm thickness of the dendrites. As described above, this is about 100 \AA and is intrinsic to the growth process. It may be related to a nonunity or a coordination-dependent sticking coefficient of the adatoms to the islands. Such assumptions have led to structure thickening in simulations while hav-

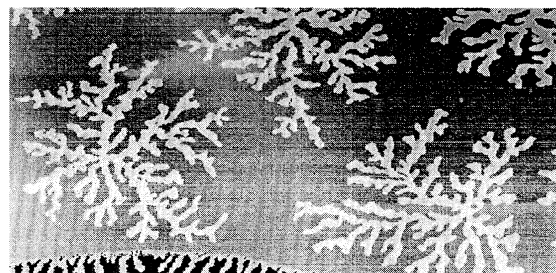


FIG. 3. Image of a film grown at room temperature with a flux of 0.2 ML/min, $\Theta = 0.3 \text{ ML}$ ($1.00 \mu\text{m} \times 0.65 \mu\text{m}$).

ing little effect on the fractal growth [7,12]. The upper limit is restricted by the size of islands. To extend this range, larger dendrites were grown by reducing the deposition flux to 0.2 ML/min. As will be discussed in more detail in a later publication, this leads to a reduced density of nuclei. Consequently, these grow to a larger size at a given Au coverage. An image of a 0.3-ML film grown under this condition is shown in Fig. 3. The linear diameter of the islands of this film is approximately 3000 to 4000 \AA . Figure 4, curve *a*, shows a plot of $\log_{10}N(r)$ vs $\log_{10}R_g$ derived from a single dendrite grown under these conditions. More than one and a half decades of power-law behavior is found. Such an analysis was also performed on single dendrites grown at 2 ML/min. A typical result is shown in Fig. 4, curve *b*. As expected, the range in which power-law behavior exists is reduced. Figure 4, curve *c*, shows an evaluation for data averaged from six dendrites grown at the lower flux rate. We con-

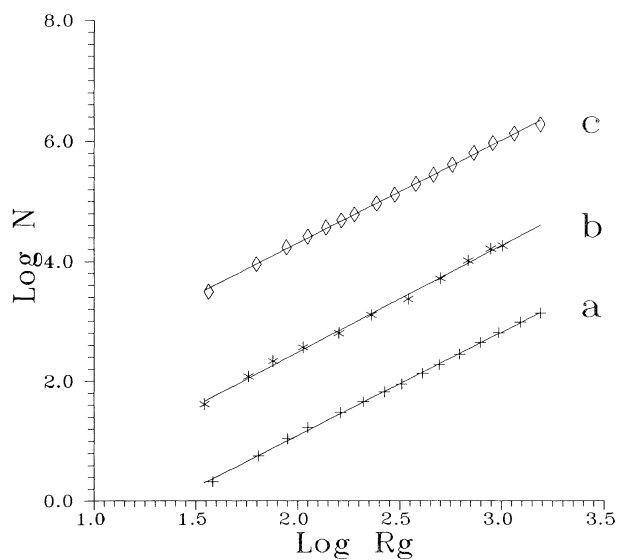


FIG. 4. Graphs of $\log_{10}N(r)$ vs $\log_{10}R_g$ from, curve *a*, single dendrite grown at 0.2 ML/min, curve *b*, single dendrite grown at 2 ML/min, and curve *c*, averaged data from six dendrites grown at 0.2 ML/min. (Offsets in the graphs are artificial.)

clude a fractal dimension $D=1.72 \pm 0.07$. This value is in excellent agreement with that determined from simulations of 2D DLA growth. Moreover, the growth must be dominated by single atoms and/or small clusters migrating via random walks with small jump lengths over the surface. Diffusion mechanisms involving either large jumps or strongly reduced adatom mobilities, leading to a percolation growth system [13], can be excluded from the large deviations from $D=1.70$ expected from the simulations of these mechanisms [6,7,9-13].

This growth mechanism should be present in other growth systems as well. The difference between the two distinct phenomena—edge and independent adatom diffusion—generally exists since the local environment of cluster edge atoms is quite different from that of free adatoms. Therefore, if there is a temperature regime in which the edge diffusion is sufficiently low while free-adatom diffusion is still appreciable, then 2D growth should obey a DLA growth mechanism under these conditions. Pronounced dendritic growth, however, requires sufficiently large defect-free regions and low densities of nuclei compared to their structural dimensions.

In conclusion, Au deposited on Ru(0001) results in two-dimensional growth in the submonolayer regime. Highly dendritic islands are formed at room temperature. The effects of annealing indicate that these shapes are thermodynamically unstable and prove a growth mechanism in which limited edge-atom diffusion is important. From a dimensional analysis of the islands, they are found to possess fractal properties with a fractal dimension $D=1.72 \pm 0.07$. This type of growth and the fractal dimension is in complete agreement with simulations

within the diffusion-limited-aggregation model. We believe this system to be an excellent example of two-dimensional DLA crystal growth.

This work was supported by the Deutsche Forschungsgemeinschaft via SFB No. 338. We also gratefully acknowledge fellowships by the Alexander von Humboldt Foundation (R.Q.H.) and the Stiftung Stipendien Fonds der Chemischen Industrie (J.S.).

-
- [1] D. D. Chambliss and R. J. Wilson (to be published).
 - [2] D. D. Chambliss, R. J. Wilson, and S. Chiang (to be published).
 - [3] P. Wynblatt, J. J. Metois, and G. C. Heyraud, *J. Cryst. Growth* **102**, 618 (1990).
 - [4] K. Yagi, K. Tobayashi, Y. Tanishiro, and K. Takanayagi, *Thin Solid Films* **126**, 95 (1985).
 - [5] G. O. Pötschke, J. Schröder, C. Günther, R. Q. Hwang, and R. J. Behm, *Surf. Sci.* (to be published).
 - [6] T. A. Witten, Jr., and L. M. Sander, *Phys. Rev. Lett.* **47**, 1400 (1981).
 - [7] T. A. Witten, Jr., and L. M. Sander, *Phys. Rev. B* **27**, 5686 (1983).
 - [8] W. Höslér, R. J. Behm, and E. Ritter, *IBM J. Res. Dev.* **30**, 403 (1986).
 - [9] D. Bensimon, B. Shraiman, and S. Liang, *Phys. Lett.* **102A**, 238 (1984).
 - [10] R. C. Ball and T. A. Witten, *Phys. Rev. A* **29**, 2966 (1984).
 - [11] P. Meakin, *Phys. Rev. Lett.* **51**, 1119 (1983).
 - [12] P. Meakin, *Phys. Rev. A* **27**, 1495 (1983).
 - [13] D. Stauffer, *Phys. Rep.* **54**, 1 (1979).

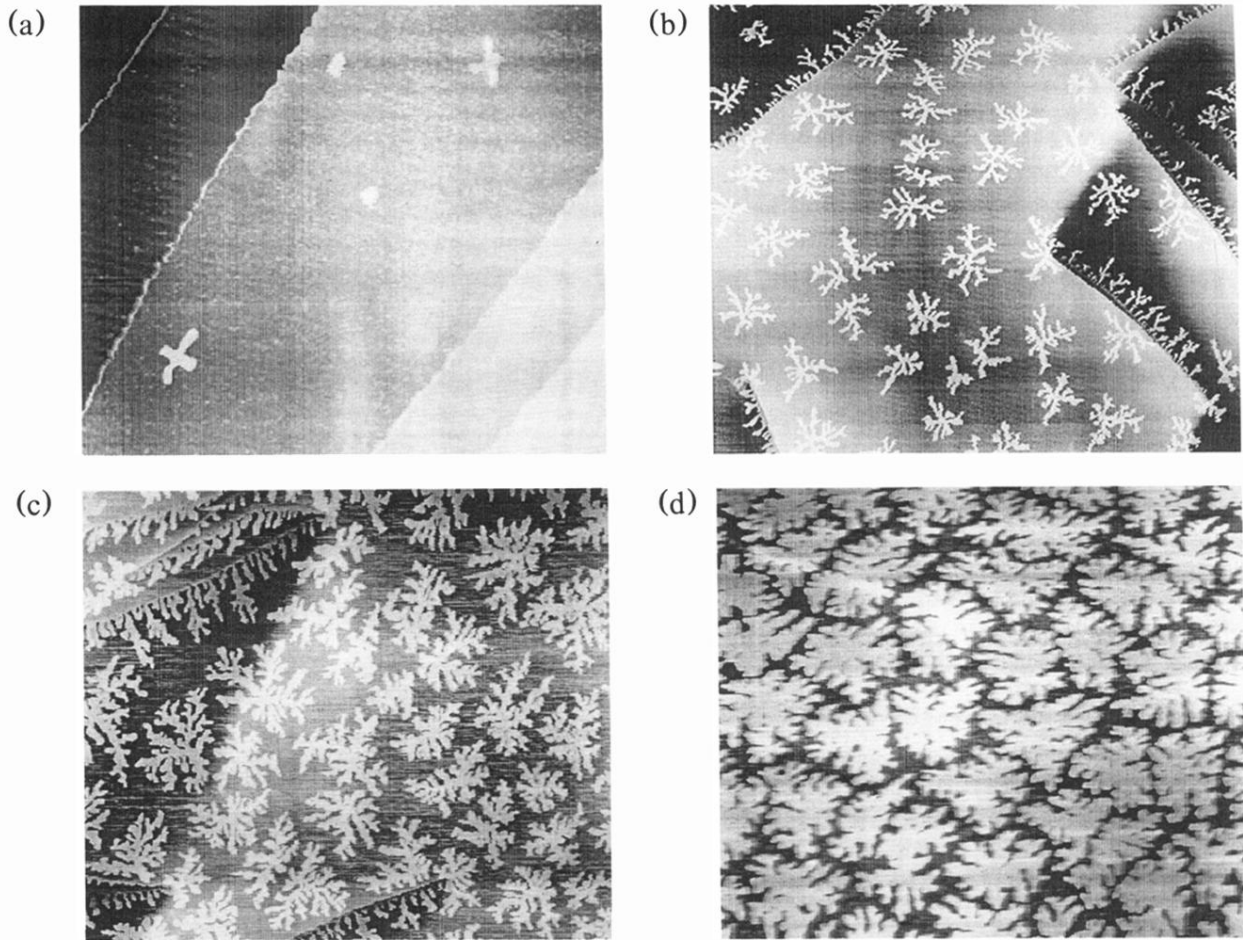


FIG. 1. Images of four films of varying coverages deposited at room temperature with a flux of 1.8 ML/min. (a) $\Theta=0.03$ ML ($0.70 \mu\text{m} \times 0.60 \mu\text{m}$), (b) $\Theta=0.15$ ML ($1.31 \mu\text{m} \times 1.20 \mu\text{m}$), (c) $\Theta=0.37$ ML ($1.13 \mu\text{m} \times 0.96 \mu\text{m}$), (d) $\Theta=0.69$ ML ($1.32 \mu\text{m} \times 1.13 \mu\text{m}$).

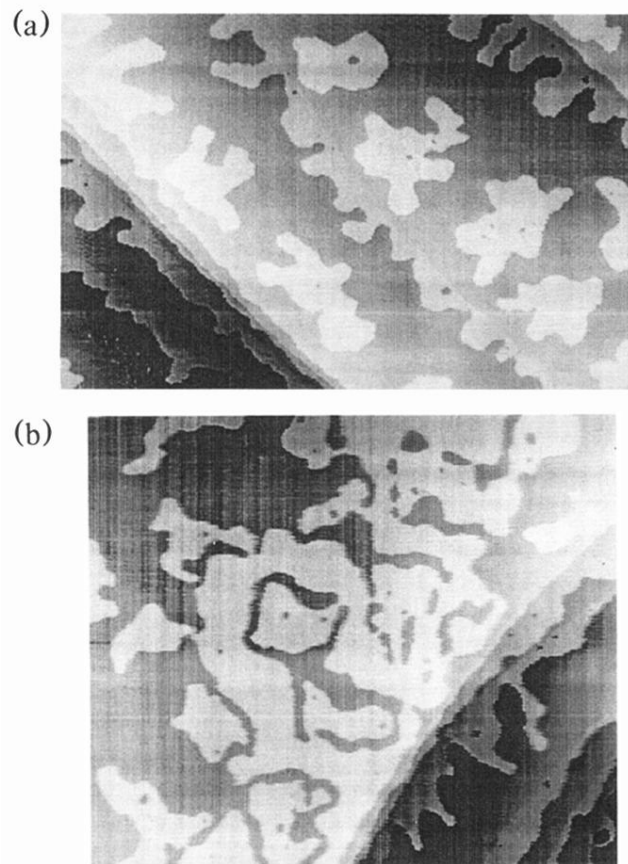


FIG. 2. Images of the identical film shown in Fig. 1(c) after annealing to (a) 650 K ($0.83 \mu\text{m} \times 0.54 \mu\text{m}$) and (b) 1100 K ($0.76 \mu\text{m} \times 0.66 \mu\text{m}$).

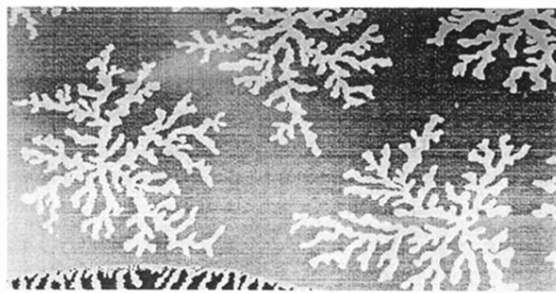


FIG. 3. Image of a film grown at room temperature with a flux of 0.2 ML/min, $\Theta = 0.3$ ML ($1.00 \mu\text{m} \times 0.65 \mu\text{m}$).